ChemComm

COMMUNICATION

View Article Online
View Journal | View Issue

Cite this: *Chem. Commun.*, 2016, 52, 8749

Received 6th May 2016,
Accepted 20th June 2016

DOI: 10.1039/c6cc03824g

www.rsc.org/chemcomm

Fully reversible three-state interconversion of metallosupramolecular architectures†

Nikita Mittal,‡ Manik Lal Saha‡ and Michael Schmittel*

The reversible switching of a sterically encumbered phenanthroline–Cu^{+}–picolinaldehyde trio back and forth between homoleptic and heteroleptic coordination using the relative metal-ion to ligand ratio is the basis for an unprecedented cyclic three-state interconversion of metallacycles.

Stimuli-responsive structural rearrangements of supramolecular architectures[1] are rapidly gaining popularity as a method to drive functional nanodevices and nanomachines.[2] In this context, the notion of clean supramolecule-to-supramolecule transformations has opened a multifaceted venue to spectacular two-state switching systems, mostly based on the (electro)-/(photo)chemical bistability of metallacycles or cages.[3] While a variety of stimuli (chemicals,[4–6] redox,[7] light,[8] concentration[9]) have been applied successfully, further improvements are needed with regard to full and quantitative reversibility, acceleration of transformations as well as access to multi-state and non-equilibrium systems.[10]

Multi-state transformations with three or more well-defined supramolecular states should be useful for creating molecular devices and logic gates of higher complexity.[11] Such transformations, though, have rarely been explored,[12] because they require multiple rearrangements of (metallo)supramolecular architectures, with each of the individual states representing a thermodynamic minimum protected by a sufficient energy barrier. Ideally, this barrier should vanish upon addition of the stimulus. Nitschke and coworkers have recently reported the cascading network of transformations of iminopyridine metal complexes, using subcomponent substitution reactions.[12] While these rearrangements are complex and unique, they represent irreversible transformations preventing their use in reversible switching processes. A three-state reversible transformation demands a design with a cyclic interconversion of the involved (metallo)supramolecules. To this end, we herein demonstrate the unprecedented and quantitative three-state cyclic interconversion of three metallacycles, namely of the square **S**, the isosceles triangle **T** and the rectangle **R**, based on the reversible switching of a sterically encumbered phenanthroline–copper(I)–picolinaldehyde trio back and forth between homoleptic and heteroleptic coordination (Scheme 1).

Conceptually, the overall processes of Scheme 1 can be viewed as three-state supramolecular transformations driven by completive *vs.* incomplete self-sorting protocols.[13] It requires the careful design of two ditopic ligands **L1**, **L2** and a metal ion M^{n+} to afford three distinct states depending on the **L1** : **L2** : M^{n+} ratio. The states involve self-sorting into a heteroleptic structure, *e.g.* $[M_4(\mathbf{L1})_2(\mathbf{L2})_2]^{4n+}$ (completive self-sorting), at **L1** : **L2** : M^{n+} = 1 : 1 : 2 and an entirely homoleptic assembly in presence of the other ligand, *e.g.* $[M_4(\mathbf{L1})_4]^{4n+}$ + 4 × **L2** (incomplete self-sorting), at **L1** : **L2** : M^{n+} = 1 : 1 : 1. In addition, a third state, *i.e.* an architecture encompassing both homoleptic and heteroleptic

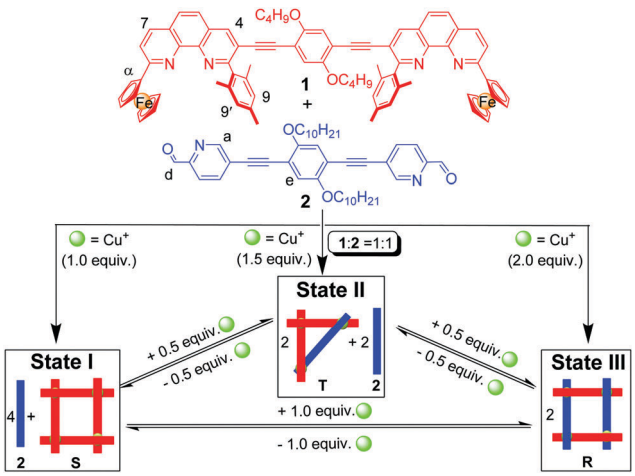

Scheme 1 Three-state cyclic interconversion of the metallosupramolecular complexes **S**, **T** and **R** depending on the Cu^{+} amount (equiv. refer to the amount of 1).

Center of Micro and Nanochemistry and Engineering, Organische Chemie I, Universität Siegen, Adolf-Reichwein-Str. 2, D-57068 Siegen, Germany. E-mail: schmittel@chemie.uni-siegen.de

† Electronic supplementary information (ESI) available: Experimental procedures and spectroscopic data are provided for all supramolecular assemblies, complexes and ligand **1**. See DOI: 10.1039/c6cc03824g

‡ Nikita Mittal and Manik Lal Saha contributed equally.

coordination motifs, is required at an intermediate metal ion's stoichiometry, again in an incomplete self-sorting (see Scheme 1, state II). The structures **R**, **S** and **T** have been chosen, because of their small number of metal complexation units, which should make (inter)conversions kinetically feasible.

To identify real binding motifs in **L1** and **L2**, one has to consider the binding constants in combination with maximum site occupancy.[14] For state I (Scheme 1), the binding constants of **L1** = **1** and **L2** = **2** should follow the order of $\log K$ ($[M(\mathbf{L1})_2]^{n+}$) ≫ $\log K$ ($[M(\mathbf{L2})_2]^{n+}$), while the heteroleptic complex $[M(\mathbf{L1})(\mathbf{L2})]^{n+}$ required in state III should be much more stable than the two homoleptic counterparts in equilibrium. To realise the three-state shuffling, the 2-ferrocenyl-9-mesityl-[1,10]-phenanthroline (**3**) (Chart 1) was selected as a prototype ligand in **L1** (*vide supra*) and tested first at the mononuclear level (Scheme 2). As established recently,[15] the encumbered ligand **3** still allows clean formation of its homoleptic complex **C1** = $[Cu(\mathbf{3})_2]PF_6$, but due to its strong electron-donating character might also cleanly furnish heteroleptic complexes with the appropriate counterparts. Ligand **3** works with both steric and donor effects, thus different from ligands in HETPHEN (heteroleptic bisphenanthroline[16]) complexes relying solely on steric factors.

Unfortunately, the heteroleptic complex **C2** = $[Cu(\mathbf{3})(\mathbf{4})]PF_6$ did not form in quantitative yield from an equimolar mixture of **3**, **4** and $[Cu(CH_3CN)_4]PF_6$ (Fig. S3, ESI†). Apparently, the stability of the corresponding pair of homoleptic complexes **C1** = $[Cu(\mathbf{3})_2]PF_6$ and $[Cu(\mathbf{4})_2]PF_6$ is partly competitive to that of the desired heteroleptic complex **C2** = $[Cu(\mathbf{3})(\mathbf{4})]PF_6$.

To realise a heteroleptic copper complex $[Cu(\mathbf{3})(\mathbf{L})]^+$ as demanded in state III′ (Scheme 2), we envisaged to utilise weaker donor ligands **L**, such as 4-methyl-*N*-(pyridin-2-ylmethylene)aniline (**5**)[17] or picolinaldehyde **6** as counterparts. The reaction of a 1 : 1 : 1 mixture of **3**, **5** and Cu^+ furnished the desired complex **C3** = $[Cu(\mathbf{3})(\mathbf{5})]PF_6$, however, still contaminated with traces of homoleptic complexes (Fig. S5, ESI†), thus suggesting a further reduction of the donor strength of **L**. We finally turned our attention to picolinaldehyde **6**[16b,18] and, indeed, a 1 : 1 : 1 mixture of **3**, **6** and Cu^+ ions furnished the heteroleptic complex **C4** = $[Cu(\mathbf{3})(\mathbf{6})]PF_6$ in a clean manner (Fig. S7, S8 and S30, ESI†). The ^{1}H NMR showed a diagnostic upfield shift of the aldehyde proton (d-H) in **C4** (δ = 9.85 ppm), which is similar to that in **C5** (δ = 9.63 ppm)[18a] and different from that in the free ligand **6** (δ = 10.08 ppm), due to the intimate π–π stacking(s) between the mesityl/ferrocenyl groups of **3** and the pyridine-2-carbaldehyde unit of **6**.

Now it was time to test whether **6** can play the desired role as an innocent bystander in state I′ (Scheme 2). A 2 : 2 : 1 mixture of **3**, **6** and Cu^+ ions afforded in an incomplete self-sorting the required state I′ = **C1** + **6** as shown by NMR data (Fig. S9 and S10, ESI†). Using ligand **6** and the complexes **C1**[15] and **C4** allowed unambiguous assignment of the ^{1}H-NMR data in state I′.

State II in Scheme 1 requires orthogonality of **C1** and **C4**.[17a] Upon mixing Cu^+ ions, ligands **3** and **6** in a 2 : 3 : 1 ratio, the ^{1}H NMR spectra of the resulting mixture showed that both **C1** and **C4** emerged in a 1 : 1 ratio, thereby confirming their orthogonality (Fig. S12, ESI†).

Subsequently, the reversibility of the interconversion of **C1** + 2 × **6** ⇌ 2 × **C4** was interrogated as a function of the metal stoichiometry (Fig. 1). Addition of 1 equiv. of Cu^+ ions (with respect to the initial amount of ligand **3**) to the solution of **C1** + 2 × **6** produced a ^{1}H NMR spectrum that precisely matched that of **C4**. When 1 equiv. of cyclam (**8**) (with respect to the initial amount of ligand **3**) was added to the resultant solution of **C4**, the initial (**C1** + 2 × **6**) state was recovered. We performed this reversible switching over three cycles and found that the transformations were completely reversible (see Fig. S11, ESI†).

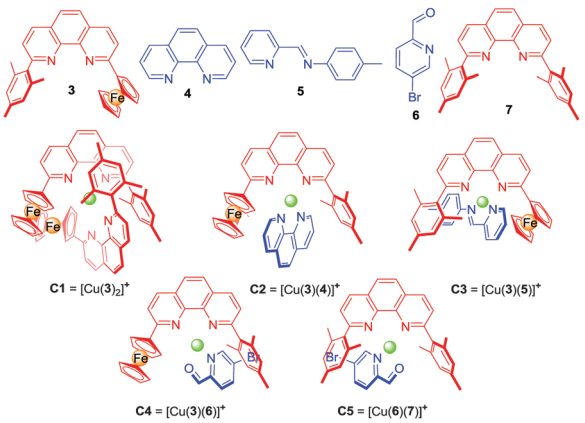

Chart 1 Ligands **3**–**7** and model complexes **C1**–**C5**.

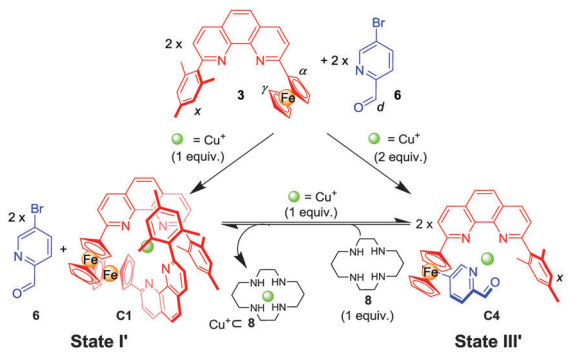

Scheme 2 Stoichiometry-controlled switching between mononuclear complexes **C1** and **C4** (all equiv. related to ligand **3**).

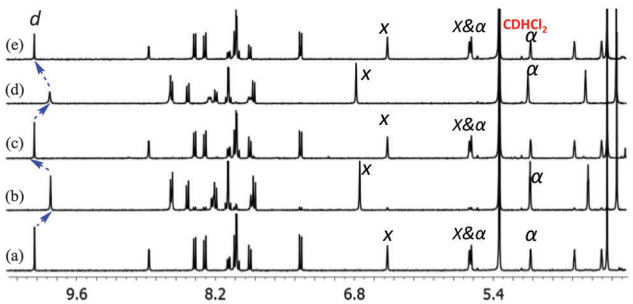

Fig. 1 Partial ^{1}H NMR spectra (400 MHz, CD_2Cl_2, 298 K) depicting the reversible switching cycles between (**C1** + 2 × **6**) and (2 × **C4**). (a), (c) and (e) correspond to (**C1** + 2 × **6**) whereas (b) and (d) represent **C4**, obtained after successive addition of Cu^+ (1 eq.) and cyclam (1 eq.). Some selected protons are assigned.

To test the three-state transformation of Scheme 1, the new ligand **1** was synthesised by means of a palladium catalyzed Sonogashira coupling reaction between 1,4-bis(decyloxy)-2,5-diiodobenzene and 3-ethynyl-2-mesityl-9-ferrocenyl-[1,10]-phenanthroline (see ESI†), both known compounds.[15] Subsequently, we prepared the supramolecular structures **S**, **T** and **R** (Chart 2) as references for the stoichiometry-controlled shuffling (Scheme 1 and Fig. 2). At first, ligand **1** and $[Cu(CH_3CN)_4]PF_6$ were mixed in a 1 : 1 ratio and refluxed for 30 min in DCM. The resultant clear red complex was characterised by ESI-MS, ^{1}H-NMR, diffusion-ordered spectroscopy (DOSY) and by elemental analysis. The ESI-MS spectrum (Fig. S32, ESI†) exhibited only two peaks at 1294.5 Da and 1774.3 Da in the region of 200–2000 Da representing **S** = $[Cu_4(\mathbf{1})_4](PF_6)_n^{(4-n)+}$ (n = 0 and 1). Therefore, the ESI-MS data suggest that square **S** is the sole product of the reaction, which was further ascertained by the DOSY NMR (see Fig. S25, ESI†) showing a single species with a diffusion coefficient of 3.4×10^{-10} m^2 s^{-1}. The structure of **S** was also confirmed by the expected ^{1}H-NMR pattern because the ferrocenyl α-H protons of **1** were split into two peaks due to their diastereotopicity in the **C1**-type of corners (see Fig. S13 and S14, ESI†). Owing to the four stereogenic axes in assembly **S**, various diastereomers are present in the ^{1}H-NMR.

Similarly, the self-assembly of $[Cu(CH_3CN)_4]PF_6$ and ligands **1** & **2** = 2 : 1 : 1 produced the rectangle **R** = $[Cu_4(\mathbf{1})_2(\mathbf{2})_2](PF_6)_4$ as the sole product. A single diffusion coefficient in the DOSY NMR ($D = 4.5 \times 10^{-10}$ m^2 s^{-1}) as well as a single set of signals in the ^{1}H-NMR provided evidence for its purity (Fig. S27 and S17, ESI†). As seen in the ^{1}H NMR, the aldehyde protons d-H of **2** in the **C4**-type complex unit in **R** appear at 9.80 ppm, thus significantly shifted upfield by 0.26 ppm compared with the free ligand **2**. Similar to model complex **C4**, the ^{1}H-NMR of rectangle **R** exhibited only one type of ferrocenyl α-H, which further confirms the heteroleptic complexation motif (Fig. S18, ESI†). The ESI-MS spectrum exhibited two peaks at m/z = 1003.5 and 1385.6 Da for $[Cu_4(\mathbf{1})_2(\mathbf{2})_2](PF_6)_n^{(4-n)+}$ for n = 0 and 1, respectively, that clearly support the integrity of R (see Fig. S34, ESI†).

Finally, the isosceles triangle **T** was prepared from a mixture of **1**, **2** and $[Cu(CH_3CN)_4]PF_6$ = 2 : 1 : 3 ratio after reflux for 1 h in acetonitrile/DCM (1 : 3). The ESI-MS spectrum shows a single major peak at 1722.7 Da for **T** = $[Cu(\mathbf{1})_2(\mathbf{2})](PF_6)^{2+}$ which suggests quantitative formation (see Fig. S33, ESI†). The formation of the isosceles triangle **T** was then further confirmed by ^{1}H-NMR, ^{1}H–^{1}H COSY NMR as well as with DOSY NMR, the latter displaying a single entity at $D = 4.3 \times 10^{-10}$ m^2 s^{-1} (Fig. S26, ESI†). In the ^{1}H-NMR, the aldehyde protons d-H of ligand **2** is diagnostically shifted from 10.09 to 9.77 & 9.74 ppm while the splitting of the ferrocenyl α-H equally suggests the presence of both homoleptic **C1**-type and heteroleptic **C4**-type corners (Fig. S15 and S16, ESI†).

The clean formation of **S**, **R** and **T** provides a reliable base for investigating the incomplete *vs.* completive self-sorting events using a varying copper(I) stoichiometry. Thus, in order to verify the shuffling as suggested in Scheme 1, first ligands **1** and **2** as well as $[Cu(CH_3CN)_4]PF_6$ were mixed in 1 : 1 : 1 ratio in CH_2Cl_2/CH_3CN to attain state I (Scheme 1). Indeed, the ^{1}H NMR of the mixture confirmed the formation of square **S** = $[Cu_4(\mathbf{1})_4]^{4+}$ while ligand **2** remained free in solution (Fig. 3a). In the ^{1}H NMR the diagnostic ferrocenyl protons of ligand **1** (α-H) split into two peaks identical to that for independently prepared square **S**, while the characteristic aldehyde proton d-H of **2** appears at the same position as in the free ligand **2** (see Fig. S20, ESI†). The DOSY NMR showed two compounds with well distinguishable diffusion coefficients, *i.e.* 3.3×10^{-10} m^2 s^{-1} (**S**) and 7.9×10^{-10} m^2 s^{-1} (**2**), in the mixture (see Fig. S28, ESI†), which confirmed the presence of state I in the mixture.

We then added 0.5 equiv. of $[Cu(CH_3CN)_4]PF_6$ (relative to **1**) to the above solution and refluxed it for 1 h to generate state II, *i.e.* triangle **T** and free ligand **2** (0.5 equiv.). The ^{1}H NMR showed two sets of aldehyde protons d-H at a 1 : 1 ratio suggesting two distinct CH=O groups, one representing the triangle **T** = $[Cu_3(\mathbf{1})_2(\mathbf{2})](PF_6)_3$ and the other the free ligand **2** (Fig. 3b), as expected for state II with its incomplete self-sorting. Comparison of the ^{1}H NMR (see Fig. S22, ESI†) of state II with that of the

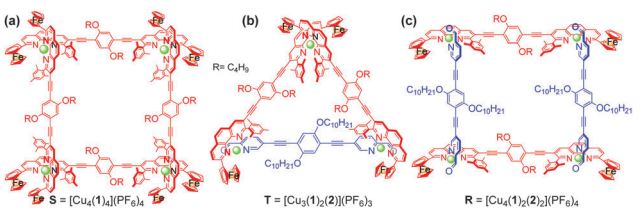

Chart 2 Chemical structures of (a) square, (b) triangle and (c) rectangle.

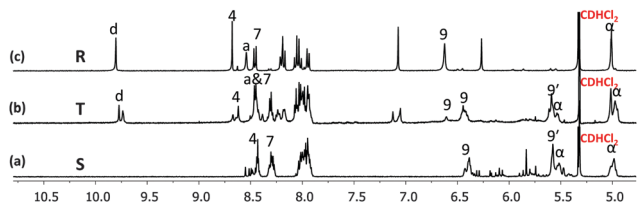

Fig. 2 Partial ^{1}H NMR spectra (400 MHz, CD_2Cl_2, 298 K) of (a) square **S**, (b) triangle **T** and (c) rectangle **R**. Selected protons are assigned.

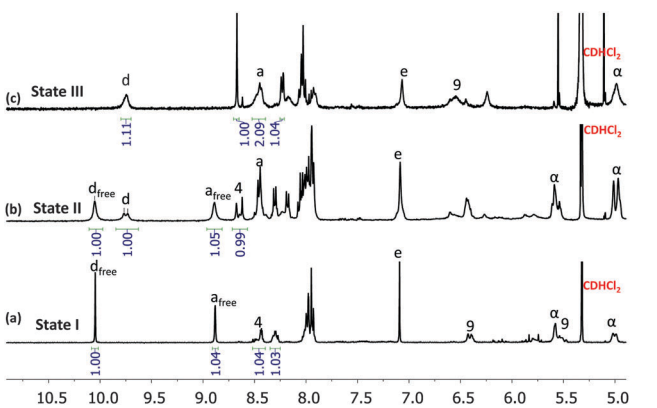

Fig. 3 Partial ^{1}H NMR spectra for comparison (400 MHz, CD_2Cl_2, 298 K) of ligand **1** and ligand **2** in 1 : 1 ratio (a) with 1 eq. Cu^+; (b) with 1.5 eq. Cu^+; (c) with 2 eq. Cu^+. Some selected protons are assigned.

independently prepared triangle **T** and ligand **2** confirmed the above assignment. The DOSY NMR (see Fig. S29, ESI†) of state II diagnostically showed two different species with $D = 4.2 \times 10^{-10}$ and 6.9×10^{-10} m^2 s^{-1} that were assigned to triangle **T** and ligand **2**, respectively. The ESI-MS (Fig. S35, ESI†) also showed one major peak of **T** and one minor peak of ligand **2** corroborating state II.

To conclude the three-state reshuffling, we added a further 0.5 equiv. of Cu^+ to the above solution and characterised it by ^{1}H NMR, ESI-MS after heating for 2 h. The ^{1}H NMR of the resultant mixture (Fig. 3c) is basically identical with the ^{1}H NMR of the pure rectangle **R**, which directly confirmed the presence of state III in the mixture.

After attaining all states of Scheme 1 in a single solution by controlling the Cu^+ ion stoichiometry, we finally tested the reversibility of this system by removing and adding Cu^+ ion. We used cyclam to remove Cu^+ ion as in our model system (Scheme 2). Confirming our design, the system turned out to be fully reversible without any loss. For example state III was easily converted into state II by just adding 0.5 equiv. of cyclam (see Fig. S24d, ESI†). Similarly states II and state III were fully switched into state I by addition of 0.5 and 1 equiv. of cyclam, respectively (see Fig. S24, ESI†). Finally, state I was converted into state II or III or sequentially from state I to state II to state III by controlling the metal ion stoichiometry (see Fig. S23 and S24, ESI†).

The MM^+ force-field calculations on square **S**, isosceles triangle **T** and rectangle **R** allow the modeling of these supramolecular architectures (see Fig. S37–S39, ESI†) and provided some insight about their structures. Taking the metal–metal distances in the energy minimised structure as a measure, the four metal corners are separated by 1.83 nm each in square **S**, in isosceles triangle three metal corners are distant by 1.80, 1.80 and 1.77 nm and again four metal corners in rectangle **R** are separated by 1.82, 1.72, 1.82, 1.72 nm.

In conclusion, we present the fully interconvertible and reversible cyclic transformation of three metallosupramolecular architectures, *i.e.* square **S**, triangle **T** and rectangle **R**. The clean and quantitative (inter)conversion of one structure into another one is the result of delicate self-sorting preferences allowing full control over homoleptic *vs.* heteroleptic *vs.* mixed homo- & heteroleptic complexation depending on metal addition/removal. To our knowledge this cycle is the first example of a fully reversible three-state transformation of supramolecular structures by varying the metal-ion : ligand ratio.

We thank the DFG (Schm 647/20-1) and the University of Siegen for continued support.

Notes and references

1 (*a*) J.-M. Lehn, *Chem. Soc. Rev.*, 2007, **36**, 151; (*b*) A. J. McConnell, C. S. Wood, P. P. Neelakandan and J. R. Nitschke, *Chem. Rev.*, 2015, **115**, 7729.
2 (*a*) A. Coskun, M. Banaszak, R. D. Astumian, J. F. Stoddart and B. A. Grzybowski, *Chem. Soc. Rev.*, 2012, **41**, 19; (*b*) U. Lüning, *Angew. Chem., Int. Ed.*, 2012, **51**, 8163.
3 (*a*) T. R. Cook and P. J. Stang, *Chem. Rev.*, 2015, **115**, 7001; (*b*) W. Wang, Y.-X. Wang and H.-B. Yang, *Chem. Soc. Rev.*, 2016, **45**, 2656.
4 Metal ion and/or ligand: (*a*) K. Harano, S. Hiraoka and M. Shionoya, *J. Am. Chem. Soc.*, 2007, **129**, 5300; (*b*) S. Hiraoka, Y. Sakata and M. Shionoya, *J. Am. Chem. Soc.*, 2008, **130**, 10058; (*c*) J. E. Betancourt, M. Martín-Hidalgo, V. Gubala and J. M. Rivera, *J. Am. Chem. Soc.*, 2009, **131**, 3186; (*d*) P. J. Lusby, P. Müller, S. J. Pike and A. M. Z. Slawin, *J. Am. Chem. Soc.*, 2009, **131**, 16398; (*e*) Y.-R. Zheng, Z. Zhao, M. Wang, K. Ghosh, J. B. Pollock, T. R. Cook and P. J. Stang, *J. Am. Chem. Soc.*, 2010, **132**, 16873; (*f*) M. L. Saha, S. Pramanik and M. Schmittel, *Chem. Commun.*, 2012, **48**, 9459; (*g*) M. L. Saha, K. Mahata, D. Samanta, V. Kalsani, J. Fan, J. W. Bats and M. Schmittel, *Dalton Trans.*, 2013, **42**, 12840; (*h*) S. Neogi, Y. Lorenz, M. Engeser, D. Samanta and M. Schmittel, *Inorg. Chem.*, 2013, **52**, 6975; (*i*) O. Jurček, P. Bonakdarzadeh, E. Kalenius, J. M. Linnanto, M. Groessl, R. Knochenmuss, J. A. Ihalainen and K. Rissanen, *Angew. Chem., Int. Ed.*, 2015, **54**, 15462.
5 Solvent: (*a*) J. Ramírez, A.-M. Stadler, N. Kyritsakas and J.-M. Lehn, *Chem. Commun.*, 2007, 237; (*b*) B. Kilbas, S. Mirtschin, R. Scopelliti and K. Severin, *Chem. Sci.*, 2012, **3**, 701.
6 Reagent: L. Zhao, B. H. Northrop and P. J. Stang, *J. Am. Chem. Soc.*, 2008, **130**, 11886.
7 Redox source: A.-M. Stadler, C. Burg, J. Ramírez and J.-M. Lehn, *Chem. Commun.*, 2013, **49**, 5733.
8 Light: (*a*) S. Chen, L.-J. Chen, H.-B. Yang, H. Tian and W. Zhu, *J. Am. Chem. Soc.*, 2012, **134**, 13596; (*b*) M. Han, R. Michel, B. He, Y.-S. Chen, D. Stalke, M. John and G. H. Clever, *Angew. Chem., Int. Ed.*, 2013, **52**, 1319; (*c*) M. Han, Y. Luo, B. Damaschke, L. Gómez, X. Ribas, A. Jose, P. Peretzki, M. Seibt and G. H. Clever, *Angew. Chem., Int. Ed.*, 2016, **55**, 445.
9 Concentration: X. Lu, X. Li, K. Guo, T.-Z. Xie, C. N. Moorefield, C. Wesdemiotis and G. R. Newkome, *J. Am. Chem. Soc.*, 2014, **136**, 18149.
10 C. S. Wood, C. Browne, D. M. Wood and J. R. Nitschke, *ACS Cent. Sci.*, 2015, **1**, 504.
11 (*a*) L. F. Lindoy, *Nature*, 1993, **364**, 17; (*b*) A. P. de Silva and S. Uchiyama, *Nat. Nanotechnol.*, 2007, **2**, 399.
12 (*a*) V. E. Campbell, X. de Hatten, N. Delsuc, B. Kauffmann, I. Huc and J. R. Nitschke, *Nat. Chem.*, 2010, **2**, 684; (*b*) W. Meng, T. K. Ronson, J. K. Clegg and J. R. Nitschke, *Angew. Chem., Int. Ed.*, 2013, **52**, 1017.
13 M. L. Saha and M. Schmittel, *Org. Biomol. Chem.*, 2012, **10**, 4651.
14 R. Krämer, J.-M. Lehn and A. Marquis-Rigault, *Proc. Natl. Acad. Sci. U. S. A.*, 1993, **90**, 5394.
15 M. L. Saha, N. Mittal, J. W. Bats and M. Schmittel, *Chem. Commun.*, 2014, **50**, 12189.
16 (*a*) M. Schmittel and A. Ganz, *Chem. Commun.*, 1997, 999; (*b*) M. L. Saha, S. Neogi and M. Schmittel, *Dalton Trans.*, 2014, **43**, 3815.
17 (*a*) M. L. Saha, S. De, S. Pramanik and M. Schmittel, *Chem. Soc. Rev.*, 2013, **42**, 6860; (*b*) Depending on the substituent in the 4-position of anilines, the association constant K_{ass} of iminopyridines towards $[Cu(phenAr_2)]^+$ ($phenAr_2$ = 2,9-diaryl-[1,10]-phenanthroline) varies from 10^4 to 10^6 M^{-1}.
18 (*a*) M. Schmittel, M. L. Saha and J. Fan, *Org. Lett.*, 2011, **13**, 3916; (*b*) J. Fan, M. L. Saha, B. Song, H. Schönherr and M. Schmittel, *J. Am. Chem. Soc.*, 2012, **134**, 150.

